

## Oxidative Damage to DNA: Counterion-Assisted Addition of Water to Ionized DNA

Robert N. Barnett,<sup>†</sup> Angelo Bongiorno,<sup>†</sup> Charles L. Cleveland,<sup>†</sup> Abraham Joy,<sup>‡</sup>  
Uzi Landman,<sup>\*,†</sup> and Gary B. Schuster<sup>\*,‡</sup>

Contribution from the Schools of Physics and Chemistry & Biochemistry, Georgia Institute of Technology, Atlanta, Georgia 30332

Received March 15, 2006; E-mail: uzi.landman@physics.gatech.edu; gary.schuster@cos.gatech.edu

**Abstract:** Oxidative damage to DNA, implicated in mutagenesis, aging, and cancer, follows electron loss that generates a radical cation that migrates to a guanine, where it may react with water to form 8-oxo-7,8-dihydroguanine (8-OxoG). Molecular dynamics and ab initio quantum simulations on a B-DNA tetradecamer reveal activated reaction pathways that depend on the local counterion arrangement. The lowest activation barrier, 0.73 eV, is found for a reaction that starts from a configuration where a Na<sup>+</sup> resides in the major groove near the N7 atoms of adjacent guanines, and evolves through a transition state where a bond between a water oxygen atom and a carbon atom forms concurrently with displacement of a proton toward a neighboring water molecule. Subsequently, a bonded complex of a hydronium ion and the nearest backbone phosphate group forms. This counterion-assisted proton shuttle mechanism is supported by experiments exploiting selective substitution of backbone phosphates by methylphosphonates.

### Introduction

The relentless oxidative assault on DNA during normal cellular metabolism and by external agents results in electron loss that causes damage having potentially lethal consequences. A frequently observed lesion is 8-oxo-7,8-dihydroguanine (8-OxoG), which is formed by the reaction of water with an oxidized guanine nucleobase in duplex DNA.<sup>1–4</sup> 8-OxoG forms a stable base pair with adenine that results in failure of the mismatch recognition mechanisms that proofread DNA, with the consequent genesis of potentially fatal G-to-T transversions.<sup>5</sup> Experimentalists and theoreticians have searched, without complete success, for a comprehensive mechanism to account for the formation of 8-OxoG. A key stumbling block is the apparent reluctance of the guanine radical cation (G<sup>•+</sup>) to combine readily with water.<sup>6,7</sup>

Experimental studies have shown that oxidation of 2'-deoxyguanosine in water solution leads to rapid deprotonation of the resulting radical cation and that subsequent reactions of the radical (G<sup>•</sup>) yield little 8-OxoG.<sup>8</sup> In contrast, oxidation of guanine-containing duplex DNA in deoxygenated buffer solution gives 8-OxoG by reaction of a base-paired guanine radical cation

with H<sub>2</sub>O<sup>3,8,9</sup> (see Figure 1). This change in reaction path highlights the importance of examining systems of sufficient compositional, structural, and environmental complexity to model faithfully the reaction of water with an oxidized guanine nucleobase in duplex DNA.

We examined computationally a 14-base-pair B-DNA oligomer [d(5'-AAGGAAGGAAGGAA-3')]/[d(3'-TTCCTTCCTTCCTT-5')] with the backbone sugar–phosphate groups, 28 Na<sup>+</sup> counterions, and a bath of water molecules (containing 804 H<sub>2</sub>O molecules). This compound contains GG segments that are known to have a relatively low ionization potential (a high hole affinity), and thus are particularly susceptible to reaction with water.<sup>10</sup> Experiments were performed on a DNA oligomer containing the same AAGGAA segments and were designed specifically to probe the effect of (negatively charged) phosphate groups on the reaction of water with oxidized DNA by their selective replacement with (neutral) methylphosphonate groups.

### Materials and Methods

**Computational Methods.** The multicomponent system studied here encompasses a large number of degrees of freedom, characterized by a broad spectrum of dynamical frequencies, interaction strengths, and bonding modes. To meet the computational challenges presented by this system, we developed methods that enable large-scale simulations of seamlessly coupled quantum mechanical (QM) and classical (molecular mechanical, MM) subsystems that allow systematic exploration of structure, bonding, dynamics, and reaction pathways. The hybrid

<sup>†</sup> School of Physics.

<sup>‡</sup> School of Chemistry & Biochemistry.

- (1) Spassky, A.; Angelov, D. *J. Mol. Biol.* **2002**, *323*, 9–15.
- (2) Burrows, C. J.; Muller, J. G. *Chem. Rev.* **1998**, *98*, 1109–1154.
- (3) Kupan, A.; Sauliere, A.; Broussy, S.; Seguy, C.; Pratviel, G.; Meunier, B. *ChemBioChem* **2006**, *7*, 125–133.
- (4) Gimisis, T.; Cismas, C. *Eur. J. Org. Chem.* **2006**, 1351–1378.
- (5) Hsu, G. W.; Ober, M.; Carell, T.; Beese, L. *Nature* **2004**, 217–221.
- (6) Reynisson, J.; Steenken, S. *Phys. Chem. Chem. Phys.* **2002**, *4*, 527–532.
- (7) Gervasio, F. G.; Laio, A.; Iannuzzi, M.; Parinello, M. *Chem. Eur. J.* **2004**, *10*, 4846–4852.
- (8) Kasai, H.; Yamaizumi, Z.; Berger, M.; Cadet, J. *J. Am. Chem. Soc.* **1992**, *114*, 9692–9694.

- (9) Ly, D.; Kan, Y.; Armitage, B.; Schuster, G. B. *J. Am. Chem. Soc.* **1996**, *118*, 8747–8748.
- (10) Senthilkumar, K.; Grozema, F. C.; Guerra, C. F.; Bickelhaupt, F. M.; Lewis, F. D.; Berlin, Y. A.; Ratner, M. A.; Siebbeles, L. D. A. *J. Am. Chem. Soc.* **2005**, *127*, 14894–14903.

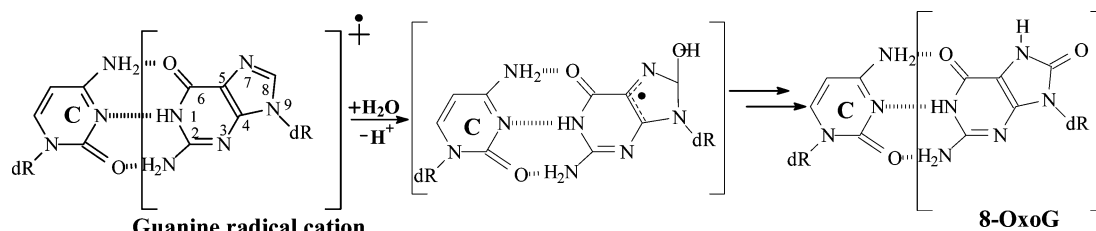


**Figure 1.** Schematic representation of the addition of water to C8 of a guanine radical cation that is base-paired with cytosine in duplex DNA and the subsequent formation of 8-OxoG.

QM/MM technique we developed<sup>11</sup> (Figure 2) employs a QM method that is particularly suited for finite systems (neutral or charged),<sup>12</sup> based on local spin-density (LSD) functional theory including generalized gradient corrections (GGA),<sup>13</sup> in conjunction with a plane-wave basis (with a cutoff energy of 62 Ry) and norm-conserving nonlocal soft pseudo-potentials.<sup>14</sup> In the MM (or molecular dynamics, MD) part, the Amber interatomic interaction potentials are used.<sup>15</sup> The water molecules are treated using the TIP3P model.<sup>16,17</sup> No cutoffs are used in our calculations for either the electrostatic or Lennard-Jones interactions. Moreover, we note that no periodic boundary conditions (pbc) are employed in our calculations (either QM or MM), and thus issues encountered in studies of charged systems using pbc do not arise.

In our simulations, the region treated quantum mechanically (the QM region) consisted of 230 QM atoms, including the two central GC base pairs of the B-DNA tetradecamer and associated sugar–phosphate groups, four Na<sup>+</sup> counterions, 32 H<sub>2</sub>O molecules, and 4 “linking atoms” used to bridge the QM region to the MM ones (on the 5′ and 3′ sides of the QM region, see Supporting Information and ref 11); the MM regions contain the rest of the atoms. This size of the QM region corresponds to 352 occupied Kohn–Sham wave functions of each spin (when using LSD calculations).

**Experimental Methods.** Nucleotide phosphoramidite and methylphosphonamidites were purchased from Glen Research (Sterling, VA). Anthraquinone (AQ) phosphoramidite was prepared as reported earlier.<sup>18</sup> The oligonucleotide sequences containing the methylphosphonates were assembled on an Applied Biosystems Expedite DNA synthesizer. Cleavage and deprotection of methylphosphonate-containing oligonucleotides were carried out according to the reported procedure.<sup>19</sup> The support was treated with a solution (0.5 mL) of acetonitrile/ethanol/ammonium hydroxide (45:45:10) for 30 min, followed by addition of ethylenediamine (0.5 mL). After 6 h, the supernatant was decanted and the support was washed twice with a 0.5 mL solution of acetonitrile/water (1:1). The supernatant and wash were combined and diluted to 15 mL with water. The pH was adjusted to 7 with 6 M HCl in acetonitrile/water (1:9) (~2 mL). The solution was desalted using a Waters C<sub>18</sub> desalting cartridge. The oligonucleotides were purified by HPLC on a Hitachi system using a C<sub>18</sub> preparative column. UV melting and cooling curves were recorded on a Cary IE spectrophotometer. CD spectra were recorded on a JASCO spectrophotometer. Both melting and CD data showed that the methylphosphonate-containing oligonucleotides, a mixture of diastereomers, exhibit B-form DNA characteristics.

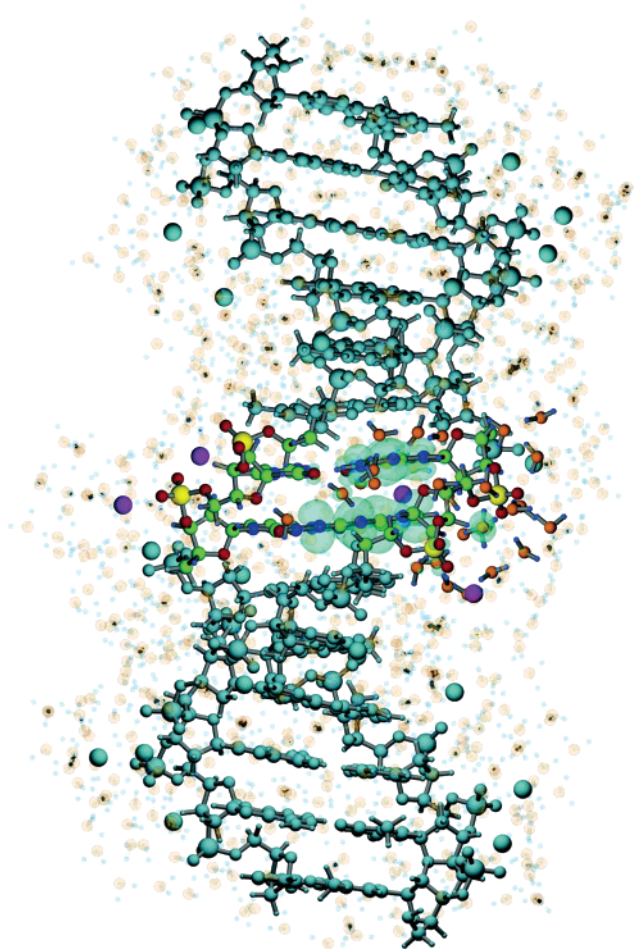


**Figure 2.** QM/MM calculation of the ionization hole in a 14-base-pair oligomer of B-DNA [d(5′-AAGGAAGGAAGGAA-3′)]/[d(3′-TTCCTTCCTTCCTT-5′)], where the bold letters denote the region treated quantum mechanically (QM). The atoms in the QM region are shown in color, and those in the classical molecular mechanics (MM) region are depicted in blue-gray; the classically treated H<sub>2</sub>O molecules are depicted as a background shadow. The hole density (electron density difference between the neutral and ionized systems, both calculated for the same geometry) is superimposed on the QM region, and it appears as the light blue isosurfaces localized on the GG step. The total number of atoms in the MM region is 3096 (12 base-pairs, 772 water molecules, and 22 Na<sup>+</sup>), and the QM region contains 230 atoms (2 base-pairs (G/C)<sub>2</sub> linked by sugar–phosphate groups, 32 water molecules, and 4 Na atoms). The number of valence electrons included in the QM calculation is 704. In the QM region, the color assignments are as follows: P, yellow; C, green; N, blue; O(base), red; O(phosphate), red; O(H<sub>2</sub>O), orange; H(H<sub>2</sub>O), small blue spheres; Na, purple. Note that most of the counterions are located in the vicinity of the phosphate groups, with one of the counterions in the QM region residing in the major groove.

- (11) Bongiorno, A.; Barnett, R. N.; Li, Y.; Suh, S. B.; Ricci, D.; Cleveland, C. L.; Landman, U. *J. Phys. Chem.*, submitted for publication (2006).
- (12) Barnett, R. N.; Landman, U. *Phys. Rev. B* **1993**, *48*, 2081.
- (13) Perdew, J. P.; Burke, K.; Ernzerhof, M. *Phys. Rev. Lett.* **1996**, *77*, 3865; **1997**, *78*, 1396(E).
- (14) Troullier, N.; Martins, J. J. *Phys. Rev. B* **1991**, *43*, 1993.
- (15) Kollman, P. A.; Dixon, R.; Cornell, W.; Fox, T.; Chipot, C.; Pohorille, A. *Computer Simulations of Biomolecular Systems*; Elsevier: Amsterdam, 1997; Vol. 3.
- (16) Jorgensen, W. L. *J. Am. Chem. Soc.* **1981**, *103*, 335.
- (17) Jorgensen, W. L.; Chandrasekhar, J.; Madura, J. D.; Impey, R. W.; Klein, M. L. *J. Chem. Phys.* **1983**, *79*, 926.
- (18) Gasper, S. M.; Schuster, G. B. *J. Am. Chem. Soc.* **1997**, *119*, 12762–12771.
- (19) Hogrefe, R. I.; Vaghefi, M. M.; Reynolds, M. A.; Young, K. M.; Arnold, L. J. *Nucleic Acids Res.* **1993**, *21*, 2031.

[ $\gamma$ -<sup>32</sup>P]-ATP was obtained from GE Biosciences, and terminal dinucleotide transferase (TDT) was obtained from New England Biolabs. Fpg was purchased from Trevigen and used according to the

protocol provided. The oligonucleotides were radiolabeled at the 3' end with [ $\gamma$ - $^{32}\text{P}$ ] and TDT. The radiolabeled DNA was purified by 20% polyacrylamide gel electrophoresis (PAGE). Samples for irradiation were prepared by hybridizing a mixture of "cold" (10  $\mu\text{M}$ ) and radiolabeled (10 000 cpm) oligonucleotides with the complementary strands in sodium phosphate buffer (pH 7). Hybridization was achieved by heating the sample at 90  $^{\circ}\text{C}$  for 3 min, followed by slow cooling to room temperature. Samples (20  $\mu\text{L}$ ) were irradiated in microcentrifuge tubes in a Rayonet photoreactor equipped with 350 nm lamps. After irradiation, the samples were precipitated with ethanol (100  $\mu\text{L}$ ) in the presence of glycogen (1  $\mu\text{L}$ , 20 mg/mL), centrifuged, washed with 80% ethanol (100  $\mu\text{L}$ ), dried, treated with Fpg, washed with water, and dried. The samples were then dissolved in loading solution (bromophenol blue in 4:1 formamide/water) and electrophoresed on a 20% 19:1 acrylamide/bis-acrylamide gel containing urea (7 M) at 70 W for 90 min. The gels were dried and the cleavage sites visualized by autoradiography. Quantization of the cleavage bands was performed on a phosphorimager.

## Results and Discussion

The path for the addition of water to oxidized guanine can be conveniently divided into three main processes: (i) an ionization event and the subsequent migration of the resulting radical cation (hole) by hopping to an appropriate reactive segment;<sup>20–22</sup> (ii) evolution of the configuration at that segment to one that enables the reaction with water, which entails overcoming an entropic barrier; and (iii) addition of water to the guanine radical cation. In this framework, the overall likelihood for reaction is determined jointly by the probabilities of hole migration, which has been widely investigated,<sup>20–23</sup> formation of reaction-susceptible configurations, and the subsequent addition of water, with the latter being the focus of the present study.

As a prelude to the mechanistic investigation, we surveyed portions of the accessible configurational space of the DNA oligomer and its solvent and counterion environment through room-temperature classical MD simulations for a 10 ns interval. From this dynamically generated ensemble, we chose several sample configurations for further inspection, with the relative stability of the selected configurations (estimated through residence-time analysis) serving as the main selection criterion. Subsequently, these configurations were ionized (an electron was removed), and the ones with the lowest vertical ionization potentials (vIP) were chosen for further relaxation. This selection process yields a small number of highly probable molecular configurations of DNA and its environment with high electron–hole affinities.

Structural relaxation of these selected ionized DNA configurations shows an energy lowering ( $\Delta_{\text{R}}$ ) of 0.4–0.5 eV; that is, the adiabatic ionization potential (aIP) is below the vIP by this amount. We find that the most significant structural change occurs in the medium surrounding the DNA molecule rather than in the DNA itself<sup>24</sup> (see Supporting Information). These changes are mainly reorientations of water molecules within a radius of 6–8  $\text{\AA}$  of the DNA that preferentially align them with the centroid of the hole distribution in the DNA. Accompanying this orientational relaxation, which maximizes the interaction

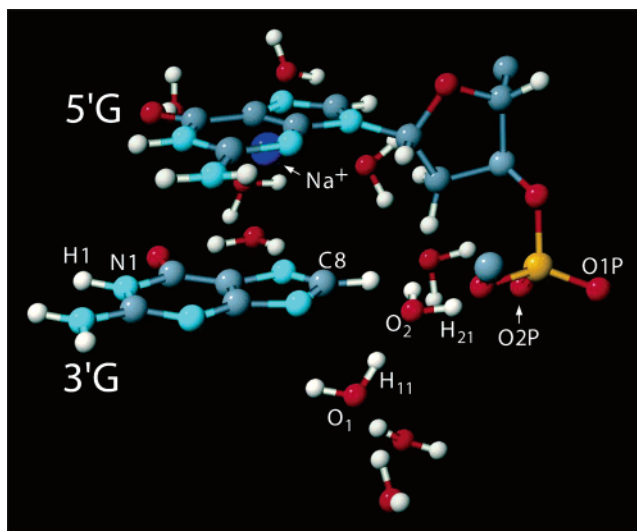


**Figure 3.** Atomic configuration of part of the DNA strand containing the GG step (see Figure 2). The  $\text{Na}^+$  (dark blue sphere) is located in the major groove in proximity of the nitrogen (N7) of the 5'-G. The color assignments are as follows: P, yellow; C, gray; N, blue; O, red; H, white. The reaction site is labeled C8 of the 3'-G, and the oxygen of the attacking  $\text{H}_2\text{O}$  molecule is O1.

between the negative end (the oxygen lone-pairs) of the  $\text{H}_2\text{O}$  molecules with the (positive) hole, is a relatively small displacement (less than 0.1  $\text{\AA}$  for the closest molecules) of the water molecules toward the hole. These motions comprise the majority contributions to polaron<sup>25</sup> stabilization in the DNA.

Figure 3 is a close-up view of the DNA at the GG step (see Figure 2) in a configuration corresponding to one of the lowest aIP observed in our simulation (aIP = 6.32 eV;  $\Delta_{\text{R}}$  = 0.53 eV). In this configuration, a  $\text{Na}^+$  is located in the major groove in proximity to the nitrogen (N7) of the 5'-G of a GG step; for reference, we label the carbon atom (C8) of the 3'-G, which is a site of attack by water (denoted as O1). After vertical ionization, the hole distribution (that is, the spatial distribution of the lowest unoccupied spin–orbital) is 38% on the 3'-G and 31% on the 5'-G. After relaxation, this distribution changes to 51% 3'- and 36% 5'-G; that is, a 30% higher hole density on the 3'-G (see Supporting Information).

It is pertinent to discuss the location of the guanine H1 proton, which participates in the hydrogen bonding that pairs G and C, and its possible influence on the reaction of water with guanine radical cation in DNA.<sup>8</sup> In solution, the guanine radical cation has a  $\text{pK}_{\text{a}}$  = 3.9 and cytosine has a  $\text{pK}_{\text{a}}$  = 4.45, which shows that the energy of the system is lowered by 0.03 eV when the H1 proton of the guanine radical cation is transferred to cytosine.<sup>26</sup> However, this situation may not pertain to ionized guanine when it is part of DNA. Indeed, our analysis reveals that the location of this proton is strongly dependent on solvation and the precise counterion configuration. Calculations on an isolated ionized GC base pair in the gas phase yield an energy difference of 0.02 eV, favoring the proton on the guanine with a transfer barrier of 0.07 eV, a result that is in correspondence with previous findings.<sup>24,27</sup> For an ionized GC base pair in DNA with the  $\text{Na}^+$  in the major groove (Figure 3), our calculations

(20) Barnett, R. N.; Cleveland, C. L.; Joy, A.; Landman, U.; Schuster, G. B. *Science* **2001**, *294*, 567–571.

(21) Schuster, G. B. *Long-Range Charge Transfer in DNA I, II*; Springer-Verlag: Heidelberg, 2004; Vol. 236, p 237.

(22) Ratner, M. A. *Proc. Natl. Acad. Sci. U.S.A.* **2001**, *98*, 387–389.

(23) Joseph, J.; Schuster, G. B. *J. Am. Chem. Soc.* **2006**, *128*, 6070–6074.

(24) Gervasio, F. G.; Laio, A.; Parrinello, M.; Boero, M. *Phys. Rev. Lett.* **2005**, *94*, 158103.

(25) Henderson, P. T.; Jones, D.; Hampikian, G.; Kan, Y.; Schuster, G. B. *Proc. Natl. Acad. Sci. U.S.A.* **1999**, *96*, 8353–8358.

(26) Candeias, L. P.; Steenken, S. *J. Am. Chem. Soc.* **1989**, *111*, 1094–1099.

(27) Ghosh, A. K.; Schuster, G. B. *J. Am. Chem. Soc.* **2006**, *128*, 4172–4173.

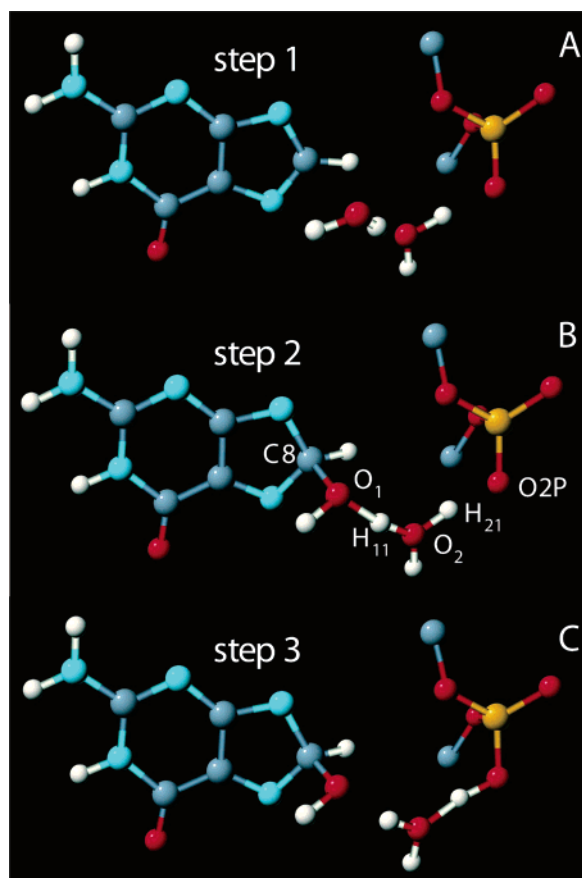


**Figure 4.** Steps of the reaction of water with the guanine radical cation in DNA. (A) Step 1: the relaxed ionized configuration. (B) Step 2: the approach of an  $\text{H}_2\text{O}$  molecule to C8 of the 3'-G, accompanied by elongation of the  $d_{\text{O}_1\text{-H}_{11}}$  bond of the molecule along the axis connecting the oxygen atom to that of a neighboring water molecule, and the activated formation of a TS complex (with a barrier of 0.73 eV, see Figure 5). (C) Step 3: further evolution of the reaction, leading to breakup of the complex, with formation of a hydroxylated G radical (8-OH-3'-G $^{\bullet}$ ) and a concomitant proton shuttle, through a Grotthuss-like process, ending with the attachment of an asymmetric hydronium group to the phosphate (with a stability gain of 0.2 eV with respect to the top of the TS barrier). The color designations are as in Figure 3.

predict a markedly enhanced stability ( $0.23 \pm 0.1$  eV) of the structure with the proton on the guanine. On the other hand, when the counterion is located near the backbone phosphate group, the calculated energy difference between the two locations for the proton is exceedingly small ( $0.0 \pm 0.1$  eV), implying a higher probability for finding it on the cytosine<sup>24</sup> than for the other location of  $\text{Na}^+$ . In the following analysis, we focus on the reaction path starting from the configuration with the  $\text{Na}^+$  in the groove and the H1 on guanine; however, starting from alternative configurations does not modify the conclusions (see below).

Analysis of the reaction mechanism, starting from the configuration shown in Figure 3, leads to identification of the steps depicted in Figure 4, where we present for clarity only the part of the system directly involved in the reaction. However, it is essential for the proper evolution of the reaction that the system contain a sufficiently large water ensemble so that stabilization of developing charged species is accurately represented.<sup>28</sup> The reaction energetics along the pathway described

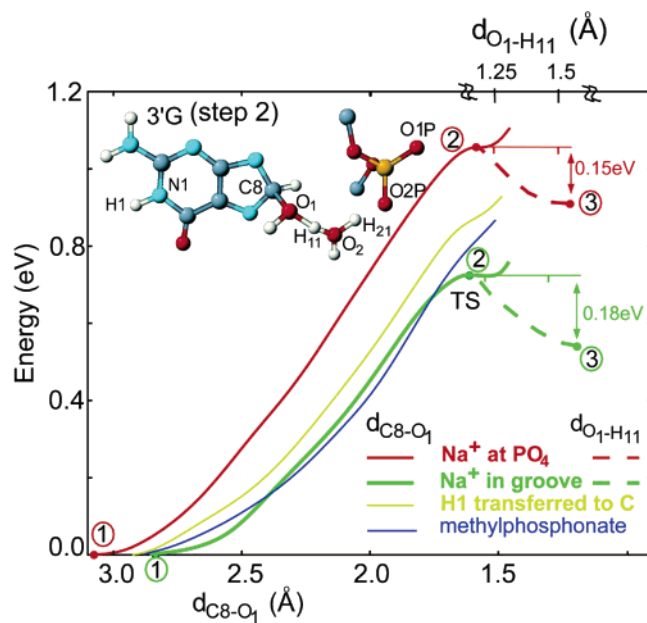


**Figure 5.** Reaction energy profiles, obtained through constrained optimizations, plotted versus the reaction coordinates (RC) for four starting configurations. The green curve corresponds to the configuration with the  $\text{Na}^+$  residing in the major groove (see Figures 3 and 4), the red one corresponds to the configuration with  $\text{Na}^+$  near the phosphate group, and the blue one gives the results for a methylphosphate (not exhibiting a saddle point). The yellow curve corresponds to a starting configuration with  $\text{Na}^+$  in the groove but H1 transferred to the cytosine, exhibiting a “weak” saddle point. For all three cases, the solid curve corresponds to  $d_{\text{C}_8\text{-O}_1}$  as the RC, and the dashed one (for the blue and red curves) corresponds to  $d_{\text{O}_1\text{-H}_{11}}$  as the RC.

in Figure 4 is given in Figure 5 (green curve); these energies and their corresponding structural parameters (see Supporting Information) were obtained by optimization of all degrees of freedom along the reaction path, except for the chosen reaction coordinate, which is constrained to prescribed values.

The first reaction step is formation of the relaxed ionized configuration; Figure 4A shows part of the relaxed configuration depicted in Figure 3, with the distance between C8 of the 3'-G and the oxygen (O1) of the nearest  $\text{H}_2\text{O}$  molecule  $d_{\text{C}_8\text{-O}_1} = 2.86$  Å, and  $d_{\text{H}_{11}\text{-O}_2} = 1.54$  Å. The reaction proceeds through the activated approach of the proximal water molecule (O1) to C8, reaching the transition state (TS step 2, Figure 4B) with a barrier ( $E_a$ ) of 0.73 eV when  $d_{\text{C}_8\text{-O}_1}$  is reduced to 1.63 Å and  $d_{\text{H}_{11}\text{-O}_2}$  is 1.13 Å. As the reaction approaches the transition state, the hole localizes on the 3'-G, reaching a value of 98% at the TS (see Supporting Information). The reaction evolves from the TS along a different primary reaction coordinate ( $d_{\text{O}_1\text{-H}_{11}}$ ), with breakup of the TS complex resulting in formation of a hydroxylated G radical (8-OH-3'-G $^{\bullet}$ ) and a concomitant proton shuttle through a Grotthuss-like process,<sup>29</sup> ending with the attachment of an asymmetric hydronium ion to the phosphate group with a stability gain of about 0.2 eV with respect to the top of the TS barrier (see Supporting Information).

For comparison with the reaction pathway where a  $\text{Na}^+$  resides in the DNA major groove in proximity to the GG segment, we show in Figure 5 (red curve) a profile of the reaction energy for the most frequently occurring configuration, where the  $\text{Na}^+$  is near the backbone phosphate group. For this configuration, the value  $\Delta P = 6.74$  eV is higher than for the

(28) Barnett, R. N.; Cleveland, C. L.; Landman, U.; Boone, E.; Kanvah, S.; Schuster, G. B. *J. Phys. Chem. B* **2003**, *107*, 3525–3537.

(29) de Grotthuss, C. J. T. *Ann. Chim.* **1806**, *LVIII*, 54–74.

case of the  $\text{Na}^+$  in the groove (6.32 eV), indicating less affinity for the hole. The relaxed hole distribution of this configuration is 42% 3'-G and 36% 5'-G, and the barrier for reaction with water is  $E_a = 1.05$  eV. The geometrical characteristics of the reaction are similar to those found for the configuration with a  $\text{Na}^+$  in the groove, despite the 0.3 eV increase in activation energy. We also considered a case where the reaction evolves from a relaxed configuration of the ionized DNA with the  $\text{Na}^+$  in the groove but with the H1 proton shifted toward the cytosine. This profile (Figure 5) starts at a higher energy structure and exhibits a "weak" saddle point 0.15 eV above the TS of the reaction path starting with the proton near the guanine. Consequently, our analysis of the path for reaction of water with ionized guanine focused on a starting configuration having  $\text{Na}^+$  in the groove and H1 close to G.

These results support our conjecture that the reaction of water with ionized guanine in DNA is controlled by the arrangement of the reactants in the vicinity of the reaction site. Here, special emphasis is placed on the location of a  $\text{Na}^+$  that localizes the hole (i.e., the orbital emptied by the ionization event) on the reaction site (C8 of the attacked guanine base, see Supporting Information), and on stabilization of a hydronium ion by a nearby phosphate group. To test the counterion-assisted proton-transfer mechanism, we explored theoretically and experimentally the consequences of selective replacement of the phosphate group linking the two bases in the ionized GG step by a methylphosphonate, where a methyl group replaces the O1P atom of the phosphate (see Figure 3). Since the methylphosphonate carries no formal negative charge, this substitution generates a "counterion-starved" region in its vicinity.

Theoretical inspection of the energy variation of the methylphosphonate system along the oxygen-C8 reaction coordinate (blue curve in Figure 5) reveals that, unlike the previously described cases, this one does not exhibit a barrier top (i.e., a transition-state complex cannot be identified), indicating that the topology of the multidimensional energy surface does not have a saddle region. We note that, in the simulations where a methylphosphonate group has replaced a phosphate, a  $\text{Na}^+$  has been removed to maintain an identical overall charge balance. Lacking a negative charge, the methylphosphonate group does not efficiently stabilize the hydronium ion as the phosphate group does. The absence of a barrier top is likely to cause the system to transform reversibly back to the initial unreacted state, which would be manifested experimentally by a reduction in reaction efficiency. This effect of methylphosphonate substitution at sites adjacent to a reactive guanine was probed experimentally.

It is well known that UV irradiation of an AQ group that is linked covalently to DNA introduces a hole that migrates through the duplex by a hopping process.<sup>25,30,31</sup> The migrating hole is trapped primarily at GG segments by the irreversible addition of water, which eventually results in conversion of a guanine to an 8-OxoG. The position of the 8-OxoG in the duplex can be identified in <sup>32</sup>P-labeled samples by gel electrophoresis and autoradiography following selective enzyme-catalyzed strand cleavage at the 8-OxoG sites. We prepared AQ-linked DNA duplexes that contain methylphosphonate groups in place of phosphates near a GG step. The effect of this substitution

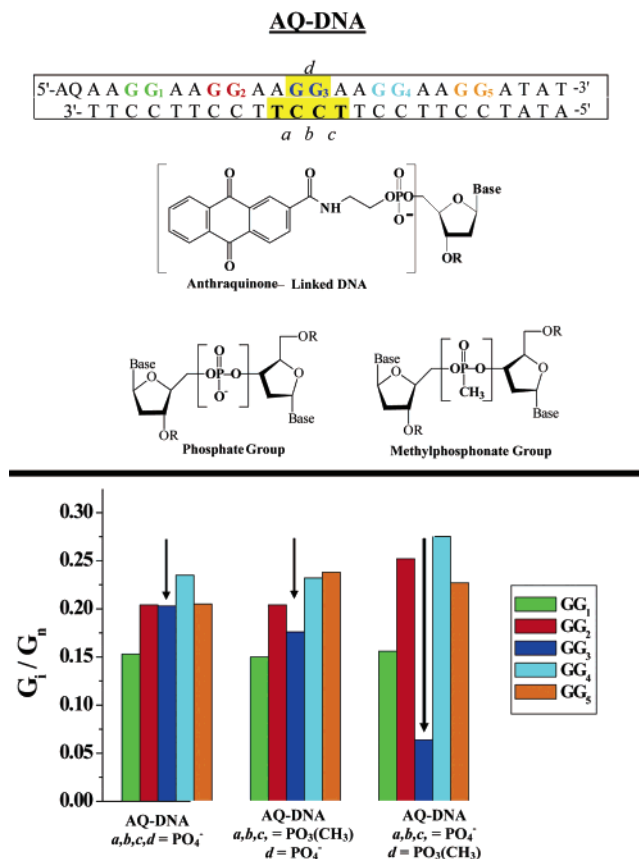


**Figure 6.** (Upper panel) AQ-DNA, a 24-mer duplex that contains an anthraquinone group linked covalently to a 5'-terminus through a four-atom tether, as shown. AQ-DNA contains five GG steps that are embedded in AGGA segments. Also shown are the linking phosphate groups at positions a, b, c, and d, surrounding  $\text{GG}_3$ , that were replaced with methylphosphonate groups. UV irradiation of AQ-DNA in buffer solution and subsequent treatment with Fpg leads to strand cleavage at each of the five GG steps. (Lower panel) Histograms of the amount of strand cleavage at each GG step. For AQ-DNA, an equivalent amount of cleavage is observed at each GG step except  $\text{GG}_1$ , which is unique because it is near to the AQ group. A similar result is observed for AQ-DNA in which the phosphate groups at positions a, b, and c are replaced by methylphosphonates. In particular, the amount of reaction at  $\text{GG}_3$  (vertical arrows) is unchanged. However, for AQ-DNA in which only the phosphate group at position d is replaced with a methylphosphonate, the amount of reaction at  $\text{GG}_3$  is significantly reduced.

supports a central role for the proximal phosphate groups in the addition of water to an oxidized guanine in DNA.

AQ-DNA (see Figure 6) contains five GG steps embedded in AGGA sequences, which is identical to the nucleobase arrangement studied by the hybrid QM/MM technique. Irradiation of AQ-DNA at 350 nm, followed by treatment of the sample with formamidopyrimidine glycosylase (Fpg),<sup>32</sup> reveals reaction and consequent strand cleavage at each of the GG steps. Figure 6 shows a histogram of reaction probabilities from an experiment carried out with AQ-DNA under single hit conditions, where each molecule reacts once or not at all. In this circumstance, the strand cleavage pattern reflects the hole probability distribution among all of the GG steps.<sup>33</sup> For AQ-DNA, there is essentially an equivalent amount of reaction at each of the five GG steps, which indicates that the rate of hole hopping is much faster than the rate of irreversible consumption by trapping. As

(30) Schuster, G. B. *Acc. Chem. Res.* **2000**, *33*, 253–260.

(31) Schuster, G. B.; Landman, U. *Top. Curr. Chem.* **2004**, *236*, 139–162.

(32) David, S. S.; Williams, S. D. *Chem. Rev.* **1998**, *98*, 1221–1261.

(33) Liu, C.-S.; Hernandez, R.; Schuster, G. B. *J. Am. Chem. Soc.* **2004**, *126*, 2877–2884.

we have previously observed, the amounts of reaction at the two guanines of the GG steps are similar because they have adenines on both their 3'- and 5'-sides.<sup>33</sup>

We modified AQ-DNA by replacing selected phosphate groups with methylphosphonates, as shown in Figure 6, where four positions of substitution are identified: three are on the strand complementary to the GG<sub>3</sub> step (positions a, b, and c), and one is at the position between the two guanines (position d). The structure of DNA is altered only slightly by substitution with methylphosphonates.<sup>34</sup> The circular dichroism spectrum of AQ-DNA is unaffected by this substitution, and the methylphosphonates change the AQ-DNA melting temperature by only 1° C. Additionally, the structure revealed by an MD simulation of the B-DNA tetradecamer described above, but with the phosphate group linking the guanine bases in the central GG step replaced by a methylphosphonate, is essentially indistinguishable from the unsubstituted case, except that the Na<sup>+</sup> population is reduced in the vicinity of the methylphosphonate. However, replacement of the phosphate group at position d with a methylphosphonate has a unique and profound effect on the reaction of ionized guanine.

The reactivity histogram shows that the substitution of three phosphate groups on the complementary strand at positions a, b, and c has little effect on the amount of reaction observed at any of the GG steps. However, replacement of the single phosphate group at position d with a methylphosphonate causes a 70% reduction in the amount of reaction at GG<sub>3</sub>, without affecting the reaction efficiency at the other GG steps. Clearly, the hole must reside at GG<sub>3</sub>, since it must pass through this position on its way from GG<sub>2</sub> to GG<sub>4</sub>, but replacement of the negatively charged phosphate group at position d with methylphosphonate uniquely inhibits reaction at GG<sub>3</sub>. This finding is consistent with the predictions made by the theoretical simulations. The addition of water to the ionized guanine becomes reversible when there is no negative charge at the nearby phosphate group to stabilize the hydronium ion, and thus the hole passes through the GG step but is rarely trapped there.

## Conclusions

The combined theoretical and experimental research described here was aimed at discovering the mechanism for the reaction

of water with oxidized DNA, which is the initiating step in the post-ionization conversion of guanine into 8-OxoG. We find that the reaction has two critical enabling features: activation of a guanine radical cation by association with a neighboring Na<sup>+</sup> counterion, and stabilization of the products by interaction of a hydronium ion with a nearby phosphate group. Elucidation of this path and the physical principles that underlie it requires an analysis that incorporates the complex, many-body nature of this condensed-phase system. The fast reorientation of water molecules (mostly those proximal to the centroid of the hole distribution) in response to nuclear motion along the reaction path implies adiabatic evolution of the reaction with respect to the reorientation molecular dynamics of the hydration environment. Such effects are common in condensed-phase reactions, and they are accentuated in this system because of the charge separation mechanism, where the shuttle of a proton (from the site of attack of the water molecule to the proximity of the backbone phosphate group) spatially separates charge from spin.

**Acknowledgment.** U.L., A.B, R.N.B, and C.L.C. gratefully acknowledge support from the U.S. Air Force Office of Scientific Research (AFOSR) and the U.S. Department of Energy (DOE). G.B.S. and A.J. are grateful for support from the National Science Foundation (NSF) and the Vassar Woolley Foundation. We thank Dr. Sriram Kanvah for assistance in the synthesis of the DNA oligomers used in this work. The computations were performed on U.S. Department of Defense computers supported by the High Performance Computing Modernization Program at DOE's National Energy Research Scientific Computing Center at the Lawrence Berkeley National Laboratory, and at the Georgia Tech Center for Computational Materials Science.

**Supporting Information Available:** Details of the QM/MM method, spatial distribution of the electron-hole, interatomic distance variations along reaction paths, and autoradiographs of PAGE gels showing the effect of methylphosphonate substitution on AQ-DNA. This material is available free of charge via the Internet at <http://pubs.acs.org>.

(34) Strauss, J. K.; Maher, J. L., III. *Science* **1994**, *266*, 1829–1834.